

## A Comparison of Crater-Size Scaling and Ejection-Speed Scaling during Experimental Impacts in Sand.

J.L.B. Anderson<sup>1</sup>, M.J. Cintala<sup>2</sup>, and M. K. Johnson<sup>1</sup>. <sup>1</sup>Department of Geoscience, Winona State Univ., Winona, MN. <sup>2</sup>Code KR, NASA JSC, Houston, TX 77058. (corresponding author: [JLAnderson@winona.edu](mailto:JLAnderson@winona.edu))

**Introduction:** Non-dimensional scaling relationships<sup>1,2,3</sup> are used to understand various cratering processes including final crater sizes and the excavation of material from a growing crater. The principal assumption behind these scaling relationships is that these processes depend on a combination of the projectile's characteristics, namely its diameter, density, and impact speed. This simplifies the impact event into a single point-source. So long as the process of interest is beyond a few projectile radii from the impact point, the point-source assumption holds<sup>2,4</sup>.

These assumptions can be tested through laboratory experiments in which the initial conditions of the impact are controlled and resulting processes measured directly. In this contribution, we continue our exploration of the congruence between crater-size scaling and ejection-speed scaling relationships. In particular, we examine a series of experimental suites in which the projectile diameter and average grain size of the target are varied.

**Data Collection Methods and Experimental Conditions:** All experiments presented here were performed with the vertical gun in the Experimental Impact Laboratory (EIL) at NASA Johnson Space Center. Ejecta were documented using an updated version of the Ejection-Velocity Measurement System (EVMS); details regarding the original EVMS are given in [5]. Since 2008, the EVMS has been updated with a 7-megapixel Nikon D100 camera yielding much higher-resolution images for analysis; the previous camera produced 1-megapixel photographs. Other optimizations to the laser geometry and computer-based analytical procedures have increased the speed at which the analyses can be completed.

Impact speeds ranged from 0.6 – 2.4 km/s; the velocity vector was always normal to the target surface. Pressure in the impact chamber was less than 1 torr. The target material was blasting sand sieved to 0.5-1 mm, giving a geometric mean grain-size of 0.71 mm. Two suites of 4.76 mm diameter spherical projectiles were used, aluminum and glass.

**Data:** The EVMS projects a "sheet" of laser light through the impact point perpendicular to the target's surface (Figure 1). The camera views the event with the detector plane subparallel to the sheet at a precisely known geometry. The laser illuminates the leading edge of the growing ejecta curtain and is strobed

at a known rate, permitting individual ejecta to be traced along their ballistic trajectories (Figure 2).

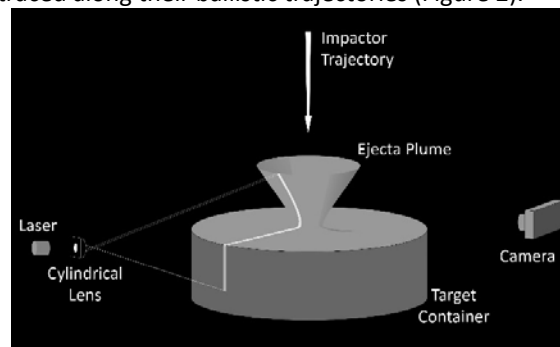


Figure 1. EVMS setup.

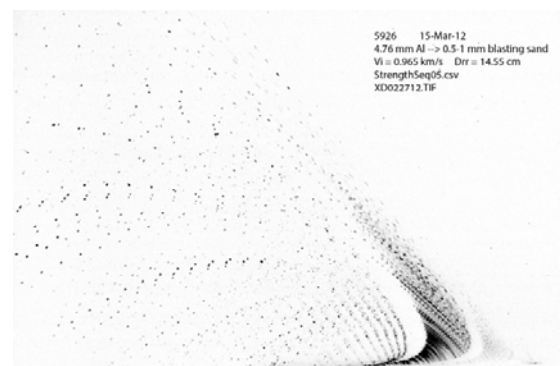


Figure 2. Example EVMS image (shown here inverted).

Individual trajectories are measured from the EVMS images and extrapolated back to the target surface, yielding ejection position, speed, and angle data for each particle. The final crater dimensions are also measured, thus permitting analysis of both crater-size and ejection-speed scaling relationships.

**Crater-Size Scaling:** Final crater dimensions have been tied to initial impact conditions through  $\Pi$ -scaling relationships<sup>2,3</sup> which infer that a single parameter  $\alpha$  is related to the slope of the  $\Pi_R$  vs.  $\Pi_2$  relationship (Figure 3). Values of  $\alpha$  derived for each suite are given in Table 1.

**Ejection-Speed Scaling:** The scaled ejection speed is related to the scaled ejection position by a power law<sup>3</sup> whose exponent  $e_x$  is a function of the crater-size scaling exponent,  $\alpha$ . These exponents and the derived values of  $\alpha$  were calculated for each individual shot; the average values for each suite are given in Table 1. Note that the  $\alpha$  values derived from the

ejection-speed scaling are higher than those from the crater-size scaling.

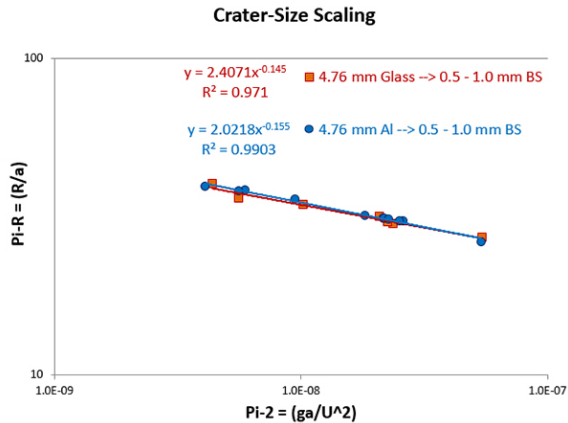


**Figure 3.** Crater-size scaling analysis for glass and aluminum suites in this study.

**Discussion:** Along with the two suites from this study, our previous work<sup>5,6,7</sup> includes three other suites of experiments in which the projectile diameter and grain size of the target were varied; values of  $\alpha$  determined from crater-size scaling and ejection-speed scaling of these suites are also given in Table 1.

The first EVMS study<sup>5</sup> initially noted that the two scaling relationships yielded different  $\alpha$  values and attributed that difference to the similarity in dimensions between the target's grains and the projectile. Subsequent EVMS studies<sup>6,7</sup> found similar discrepancies between the crater-size and ejection-speed values for  $\alpha$ . Scaling results obtained using Particle Imaging Velocimetry (PIV) and a much finer grained target<sup>8</sup>, however, showed much better agreement between the two values of  $\alpha$  (Table 1).

To examine whether this variation in  $\alpha$  might be a result of the target's granularity, we defined a parameter,  $\gamma$ , to be the ratio of the projectile diameter to the mean dimension of the grains composing the target<sup>7</sup>; that value is given for all experimental suites in Table 1. The higher-resolution camera permits de-

tailed analysis of much finer-grained targets than was possible previously, thus increasing the range in  $\gamma$  available for EVMS study.

The derived values of  $\alpha$  as a function of  $\gamma$  for the six experimental suites are shown in Figure 4. Crater-scaling values are all near the theoretical minimum. However, at small  $\gamma$  (similar sized projectile and target grains), the values derived from the ejection speeds are much higher. As  $\gamma$  increases, the ejection-speed values appear to converge with the crater-scaling values, as expected for a continuous material. It is notable that this trend appears to be independent of projectile material. Future work will attempt EVMS analysis of an even finer-grained target material to achieve larger  $\gamma$  values for direct comparison with the results of the PIV study<sup>7</sup>.

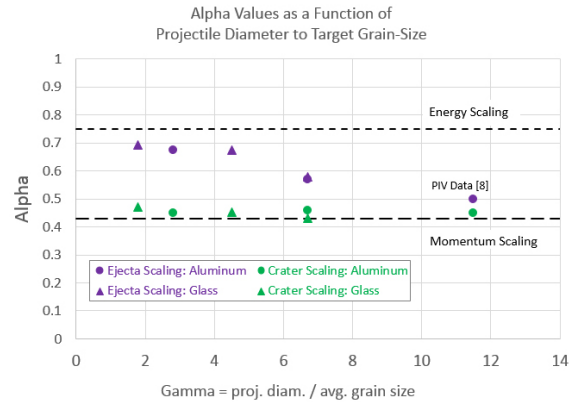


**Figure 4.** Variation of  $\alpha$  with  $\gamma$ .

**Implications:** While the assumption is commonly made that a planetary-scale target surface would present a uniform continuum to the incoming projectile, more and more high-resolution images are showing the diversity of surfaces and the number of fragments embedded in regoliths. Such large fragments may present complexities in subsurface structure that could violate the point-source assumption inherent to crater-scaling relationships.

**TABLE 1.** Comparison of alpha values determined through ejection-speed scaling and crater-size scaling methods.

Projectile (spheres)	Target	Gamma	Ejecta-Scaling Alpha	Crater-Scaling Alpha	Ref.
4.76 mm Aluminum	0.5-1 mm blasting sand	6.7	0.57 (avg.)	0.46	This study
4.76 mm Glass	0.5-1 mm blasting sand	6.7	0.58 (avg.)	0.43	This study
4.76 mm Aluminum	1-3 mm blasting sand	2.8	0.673 (avg.)	0.45	[5]
3.18 mm Glass	0.5-1 mm blasting sand	4.5	0.675 (avg.)	0.45	[6]
3.18 mm Glass	1-3 mm blasting sand	1.8	0.692 (avg.)	0.47	[7]
6.35 mm Aluminum	0.55 mm sand	11.5	0.50	0.45	[8]

**References:** [1] Chabai A.J. (1965) *JGR* 70, 5075. [2] Holsapple K.A. and Schmidt R.M. (1982) *JGR* 87, 1849. [3] Housen *et al.* (1983) *JGR* 88, 2485. [4] Holsapple K.A. and Schmidt R.M. (1987) *JGR* 92, 6350. [5] Cintala M.J. *et al.* (1999) *MAPS* 34, 605. [6] Anderson J.L.B. *et al.* (2007) *LPSC* #2266. [7] Anderson J.L.B. *et al.* (2010) *LPSC* #2084. [8] Anderson J.L.B. *et al.* (2003) *JGR* 108, doi:10.1029/2003JE002075.